# INTERACTION OF HYDROGEN JETS WITH HOT SURFACES

**A. Kessler armin.kessler@ict.fraunhofer.de**
**Phone +49 721 4640-301 Fax +49 721 4640-800301,**
**C. Wassmer, A. Koleczko, S. Knapp, V. Weiser,**
**A. Raab, N. Eisenreich**

Fraunhofer ICT, Joseph-von-Fraunhofer Str. 7, 76327 Pfinztal, Germany

## Abstract

The formation of hydrogen jets from pressurized sources and its ignition when hitting hot devices has been studied by many projects. The transient jets evolve with high turbulence depending on the configuration of the nozzle and especially the pressure in the hydrogen reservoir. In addition the length of the jets and the flames generated by ignition at a hot surface varies. Parameters to be varied were initial pressure of the source (2.5, 10, 20 and 40 MPa), distance between the nozzle and the hot surface (3, 5 and 7 m) and temperature of the hot surface (between 400 and 1000 K). The interaction of the hydrogen jets is visualized by high-speed cinematography techniques which allow analysing the jet characteristics. By combination of various methods of image processing, the visibility of the phenomena on the videos taken at 15 000 fps was improved. In addition, high-speed NIR spectroscopy was used to obtain temperature profiles of the expanding deflagrations. The jets ignite already above 450 K for conditions mainly from the tubular source at 40 MPa. In addition, the propagation of the flame front depends on all three varied parameters: temperature of the hot surface, pressure in the reservoir and distance between nozzle and hot surface. In most cases also upstream propagation occurs. A high turbulence seems to lead to the strong deflagrations. At high temperatures of the ignition sources, the interaction leads to fast deflagration and speeds up- and downstream of the jet. The deflagration velocity is close to velocity of sound and emission of pressure waves occurs.

## 1 Introduction

Hydrogen storage occurs mainly by high pressure in cryogenic tanks or by hydrides and induces specific safety issues [1]. The flame velocities of jet fires from ruptured tanks and tubes, as well as from pressurized storage [1-6] or cryogenic tanks [7, 8] are moving gas explosions depending on various parameters. The most important roles play the configuration of the nozzle and especially the pressure in the hydrogen reservoir. The temperature of the igniting device and the distance between nozzle and ignition device [9-12] give rise to theoretical approaches [13-16] and are topic of practical use [17]. The details of gas jet interaction with hot surfaces are still an interesting objective and induce scientific input to theoretical studies and also to practical applications. Depending on the properties of release and the mixture with air or oxygen determine the subsequent effects. The explosive reactions occur in wide ranges of fuel/oxidizer compositions with flame velocities of more than 100 m/s [18, 19]. The flame velocities are strongly enhanced by turbulence, especially in spherical explosions. The mechanisms for this effect are not fully understood, but turbulence is often assumed to be responsible, especially turbulence generated by the propagating flame front.

The above mentioned effects were investigated using hydrogen air jets varying the initial pressure of the source – 2.5, 10, 20 and 40 MPa, the distance from the nozzle – 3, 5 and 7 m and the temperature – 400 -1000 K of the igniting device (glow plug). The flame propagation was observed by high-speed video technics with 15 000 fps and time resolved spectroscopy in the NIR spectral range with a time resolution up to 1754 spectra/s. Ignition, flame contours, pressure wave propagation, reacting species and temperatures were evaluated. The evaluation used image processing methods, enhancing the contrast, brightness subtraction and 1-dimensional image contraction to obtain traces of all movements [6, 7, 25].

## 2 Experimental setup and data evaluation

The experimental setup Fig. 1 (photos) and Fig. 2 (scheme) was established at the open air experimental plant building of Fraunhofer ICT (Fig. 1 left) to generate turbulent transient jets. It consists of gas supply system with a pressure reservoir of a volume of ~5 L, which enables hydrogen storage at pressures up to 40 MPa and a concrete wall as a background for the jet investigation. In a perpendicular distance to the jet of 6 m a Phantom V710 high-speed camera with a 24 kW illumination system and an Avantes NIR Spectrometer (AvaSpec-NIR256-2.5TEC) were adapted to the experimental setup (see Fig. 2).

**Figure 1: Open air experimental plant buliding of Fraunhofer ICT with the high pressure storage tube (l.) and the concrete wall, here with an ignited jet in front of it (r.).**

The high pressure storage tube is operated using a fully remote-controlled compressor system. It ensures safe operation even in black-out situations by safety positions of spring-loaded valves for depressurization of the high-pressure tube, the hydrogen supply and the driving air interruption. The high-pressure storage tube is opened by a rupture disc at defined pressures (2.5, 10, 20, 40 MPa).

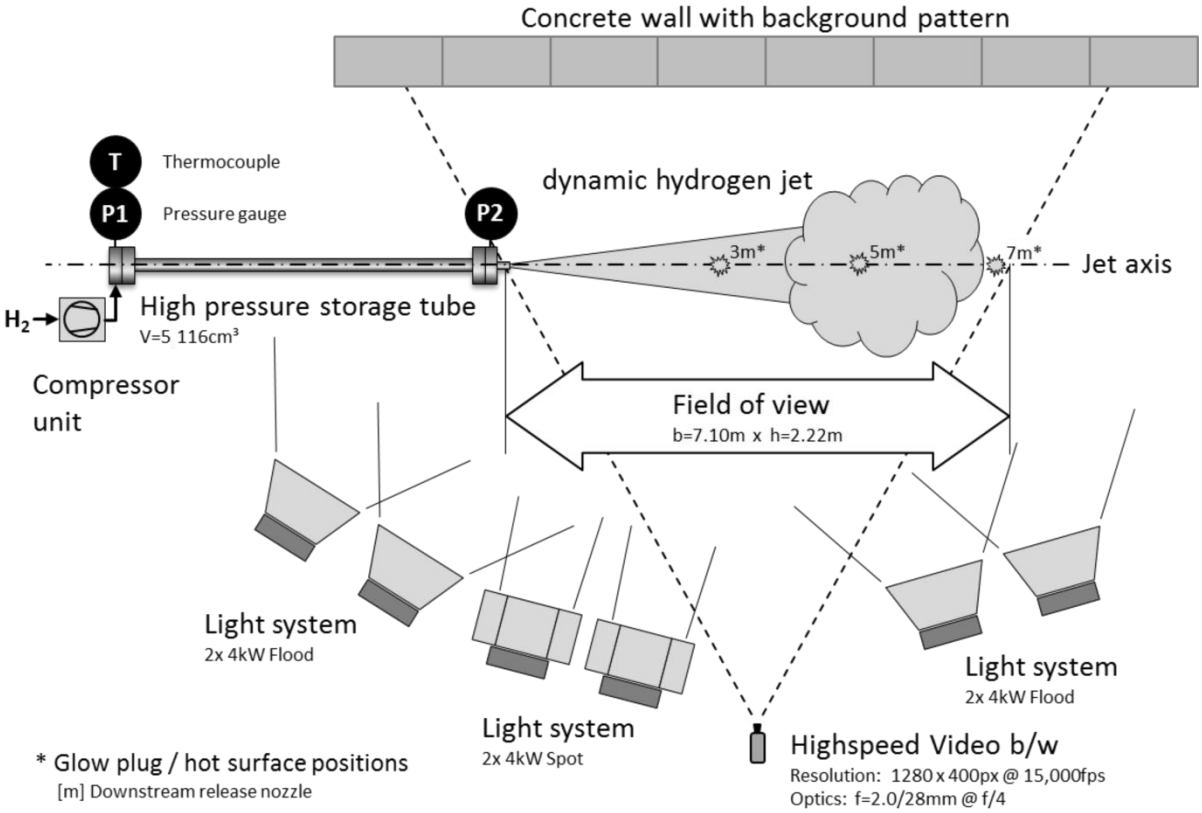


**Figure 2: Scheme of the setup.**

**Table 1: Measured release conditions**

| Nominal pressure [bar] | Activation pressure [MPa] | $t_{90-10}$ [s] | Initial pressure decay [bar/s] | Averaged pressure decay [MPa/s] | Initial gas temperature [°C] |
|---|---|---|---|---|---|
| **25** | 2.82±0.09 | 0.225±0.000 | 310.9±10 | 9.52±0.3 | 12.8±0.1 |
| **100** | 10.56±0.29 | 0.218±0.000 | 1350±37 | 37.6±1 | 12.3±0.3 |
| **200** | 22.26±0.58 | 0.200±0.004 | 3206±97 | 83.7±2.5 | 11.4±0.4 |
| **400** | 40.92±1.21 | 0.180±0.003 | 6739±233 | 170.3±6.2 | 9.1±1.2 |

The high-speed video acquisition was performed using the sub-frame capability of the Phantom V710 high-speed camera. Acquisition speed could be increased up to 15 000 fps at reduced resolution of 1280 x 400 px. As background for the recorded video, a mechanically stable modular concrete wall was applied. The wall was painted in white colour and stamped with an irregular black dot pattern to allow high-speed video analysis of both, ignited and unignited jets under identical conditions. Together with the in total 24 kW illumination system, exposure times for a single frame of 7 µs could be realized.

The single frames of the high-speed videos were evaluated with various techniques of image processing. This is necessary especially for pure hydrogen jets and flames because they are nearly invisible in the visual spectral range. First, the BOS method was applied to the recorded high-speed videos. The BOS method uses a standard method of image processing, the cross correlation of neighboured images. It was proposed by the DLR Göttingen for the application to fluid dynamics [21, 22] and introduced to hydrogen research by Fraunhofer ICT [23]. This procedure makes also very small effects in fluids visible, which are generated by fluctuations in density. Fig. 3 shows the results of two selected unignited 40 MPa experiments, which were evaluated using the BOS method to evaluate the jet head propagation on the jet axis.

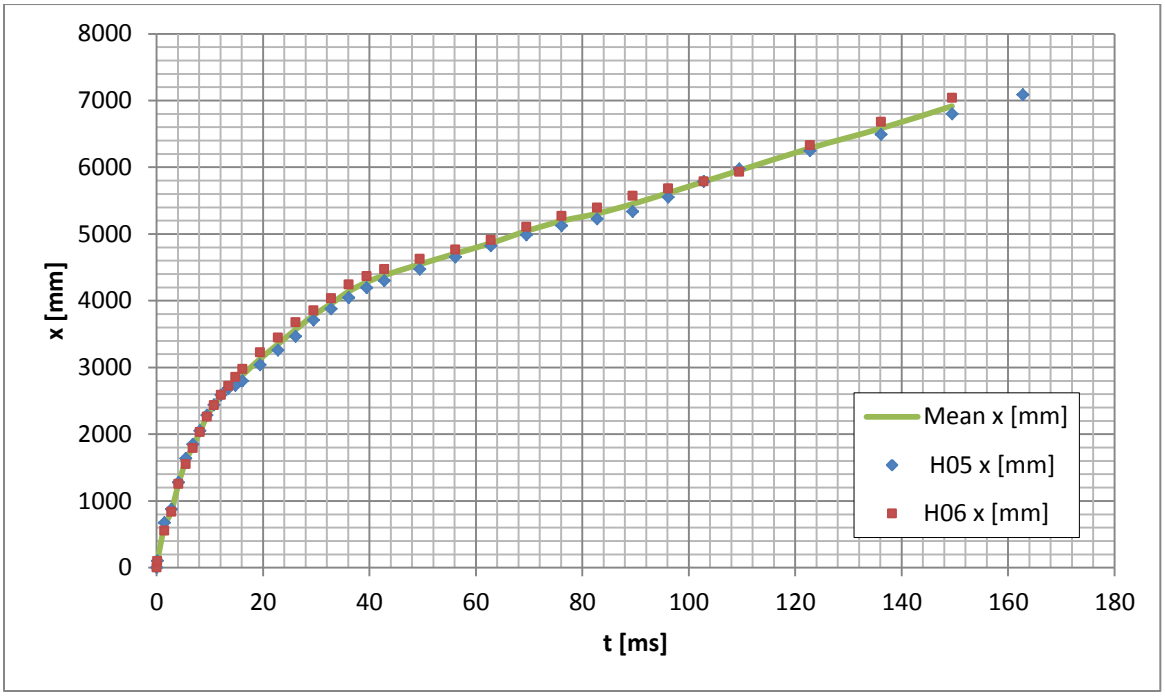


**Figure 3: Propagation of jet head front for two unignited 40 MPa experiments.**

In order to analyse further jet characteristics, the combination of various methods of image processing were applied especially to improve the visibility of effects on the videos. The steps of image processing occur by similar procedures as in Ref. [21, 25]. First, the contrast was enhanced which

enables further evaluation of the jet structures. Then the difference of the actual frame and the first frame was calculated. Finally a compacting of one dimension perpendicular to the direction of movement was performed to reduce the 3D image sequence to a 2D image of the non-compacted dimension and the time. This procedure creates an overview of the expanding jet and a possible explosion in the main direction of propagation.

The individual images of hydrogen videos are very noisy and make evaluations more difficult. Further image processing can visualize the nearly invisible hydrogen jets and subsequent flames. It uses despeckle techniques, like summing up some pixels around the actual pixel and setting small resulting pixels to zero.

The time resolved spectroscopy was carried out using available equipment which consists of a fast scanning near infrared (NIR) spectrometer to analyse the $H_2O$ bands in the spectral range between 1.3 to 2.1 µm (Avantes AvaSpec-NIR256-2.5TEC). The spectra analysis uses the least squares fit method which fits the model spectrum of calculated $H_2O$ band system spectrum to experimental spectra. The resulting fit parameter is the temperature of the $H_2O$ band system.

# 3 Results and discussion

## 3.1 Overview

The classification of the results based on the criteria of observed flame speeds and pressure records and uses “no”, “weak” (flame speed < 30 m/s) and “strong” ( >30 m/s) reactions. The “weak” reaction is further divided into a “weak” reaction and a “normal” reaction, which is in its effects close to a spherical, premixed hydrogen air explosion. An overview of the results is given in Tab. 2-4.

Despite some discrepancies the results in the tables show that high temperatures and pressures at small distance lead to “strong” reactions. Turbulence mainly induced by high reservoir pressure is obviously a reason for “strong” reactions. Longer distances dilute the hydrogen air mixture and attenuate the reaction. The entrained air can be estimated by analysing the $CO_2$ emission at 4.2 µm [25].

**Table 2: Overview of the results of performed experiments with glow plug ignition in 3 m distance at stated temperatures (X = strong reaction, O = weak reaction, H = no reaction).**

**Distance 3m**

| Pressure \ Temperature | 450 °C | 550 °C | 650 °C | 750 °C | 850 °C | 950 °C |
|---|---|---|---|---|---|---|
| 2.5 MPa | | | H44/H | H43/O | H42/O | H41/O<br>H45/O<br>H46/O |
| 10 MPa | | | H56/H<br>H57(700°C)/H | H55/O | H54/O | H53/O |
| 20 MPa | | | | H77/H<br>H78/H | H76/O | H74/X |
| 40 MPa | | | H48/H | H49/O<br>H50/O | H51/X | H52/X |

**Table 3: Overview of the results of performed experiments with glow plug ignition in 5 m distance at stated temperature (X = strong reaction, O = weak reaction, H = no reaction).**

**Distance 5m**

| Pressure \ Temperature | 450 °C | 550 °C | 650 °C | 750 °C | 850 °C | 950 °C |
|---|---|---|---|---|---|---|
| 2.5 MPa | | | | | | H40/H |
| 10 MPa | | | H61/H<br>H62(700°C)/H | H60/O | H59/O | H58/O |
| 20 MPa | | | H66/H<br>H67(700°C)/H | H65/O | H64/O | H63/O |
| 40 MPa | H24/H | H33/H | H34/H | H35/O | H37/X | H23/X |

**Table 4: Overview of the results of performed experiments with glow plug ignition in 7 m distance at stated temperature (X = strong reaction, O = weak reaction, H = no reaction).**

**Distance 7m**

| Pressure \ Temperature | 450 °C | 550 °C | 650 °C | 750 °C | 850 °C | 950 °C |
|---|---|---|---|---|---|---|
| 2.5 MPa | | | | | | |
| 10 MPa | | | | | H69/H | H68/O |
| 20 MPa | | | H73(700°C)/OH | H72/O | H71/O | H70/O |
| 40 MPa | H25/H | H26/H | H27/H | H29/O | H30/O | H32/O |

### 3.2 High-speed image sequences and evaluation

For presentation one experiment was selected from each type of reaction. Reactions of the same type gave similar results as those described here.

#### 3.2.1 "Strong" reaction

The "strong" reaction to be presented in more detail was initiated by a jet from a 40 MPa reservoir and an ignition by a glow plug with a temperature of 850 °C in a distance from the nozzle of 3 m (see Table 2, H51). The jet expands strongly behind the nozzle exit which already gives a shock wave by the rupture disk or the expansion(see Fig.4).

**Figure 4: Despeckled image of the evolving jet shortly after release and the propagating shockwave (length 3.8 m).**

The jet propagates and expands as expected by an angle of 12° and forms a vortex at the head as shown by Fig. 5 [26].

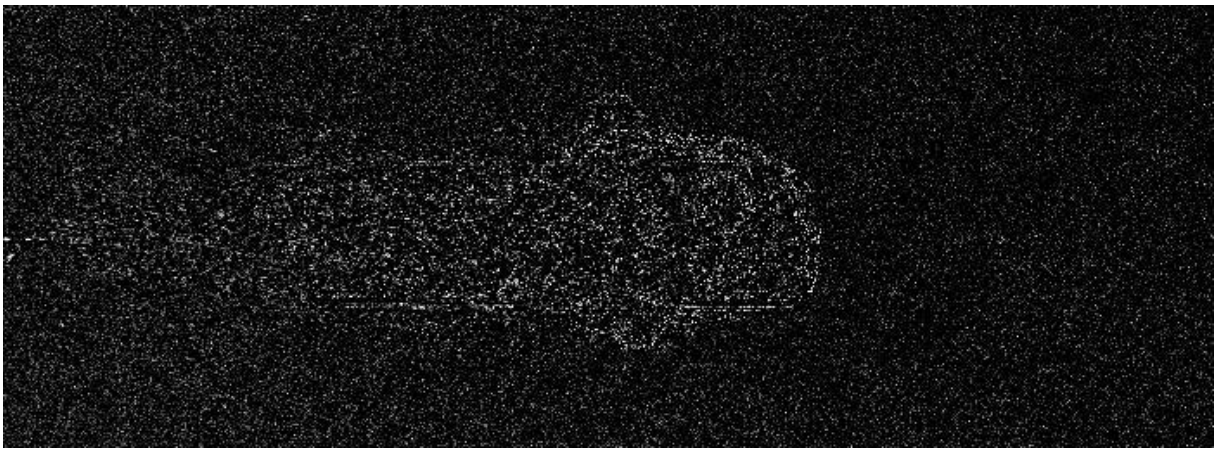

a)

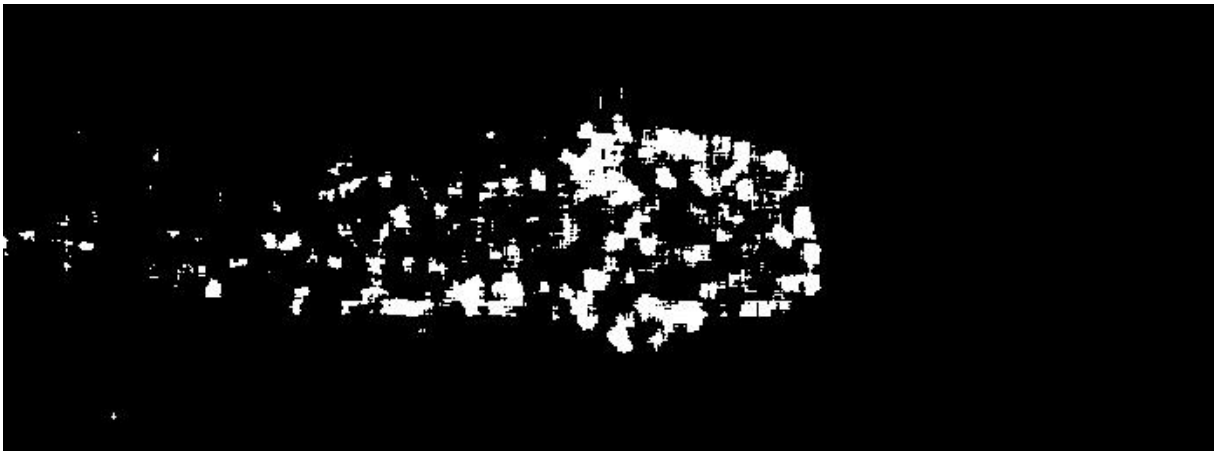

b)

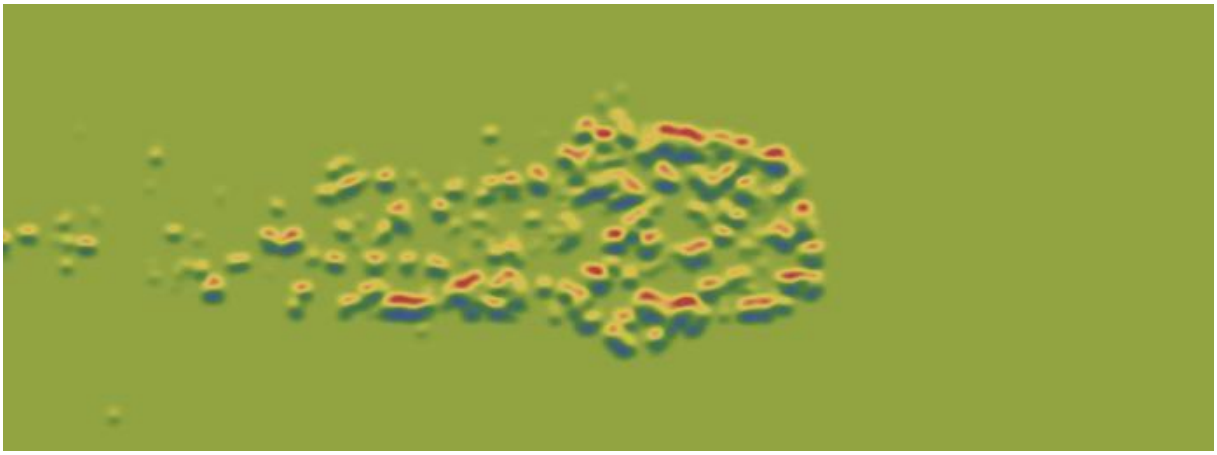

c)

**Figure 5: Sequence of images (jet after 0.01666 s) on steps of processing (a) contrast enhancement and subtraction of the first image, (b) despeckled, (c) blurred and Gaussian filter applied – colorized.**

After 0.0333 s the jet covers the glow plug and reacts with a delay of 0.001-0.002 s. Fig. 6 shows the reaction after 0.0333 s. Non-reacted parts of the jet move on and forms the later medium for the gas explosion. The reaction proceeds and emits a shock wave as evident from Fig. 6.

a)

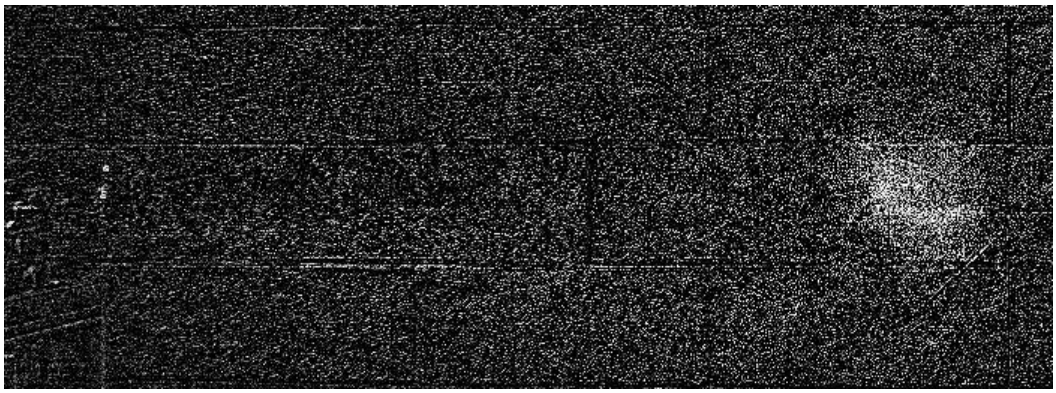

b)

c)

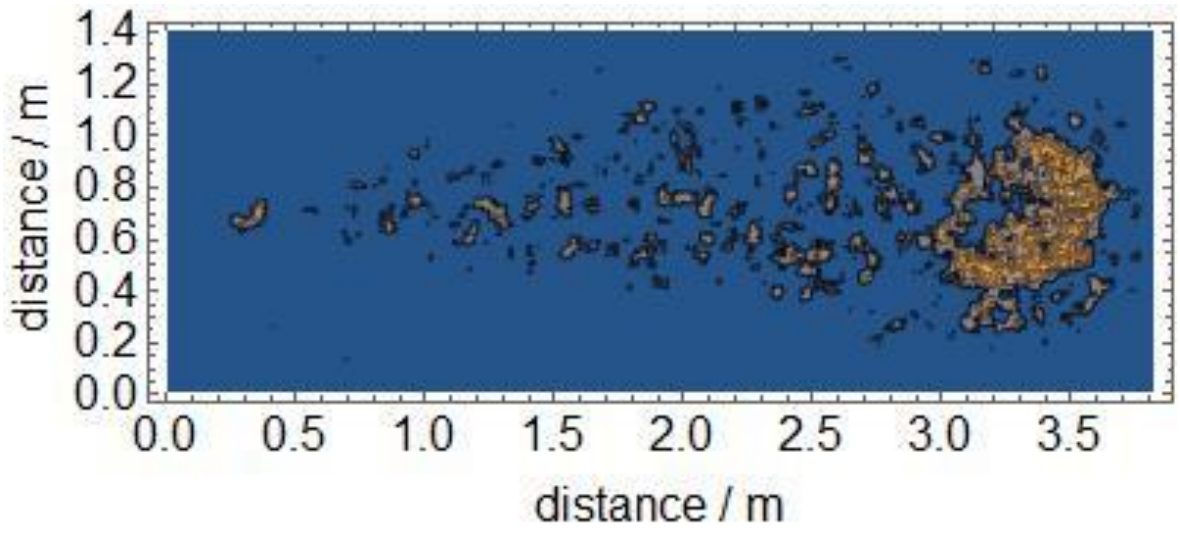


**Figure 6: Sequence of images of the jet after 0.0333 s on steps of image processing (a) contrast enhancement and subtraction of the first image, (b) despeckled, (c) contour plot with dimensions.**

A difference image from images at a time difference of 0.666 ms shows the movement of the explosion and the propagation of the shock wave. From Fig. 7 (c) or (d) the velocity of the explosion can be estimated from the difference of the radii of the rings and the time difference.

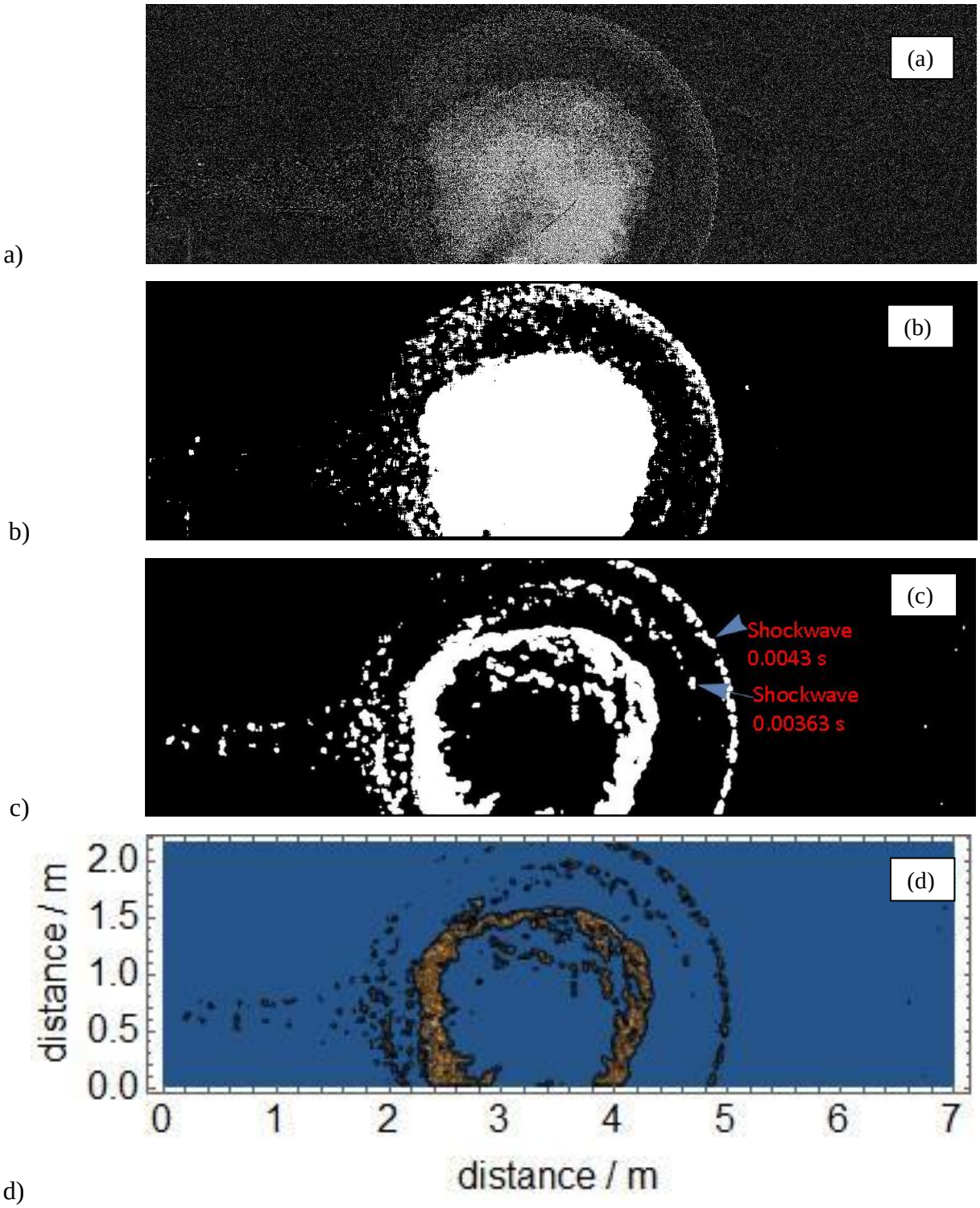


**Figure 7: Sequence of images (jet after 0.0333 s on steps of image processing (a) contrast enhancement and subtraction of the first image, (b) despeckled, (c) blurred transfer of image to data – colorized. (d) Contour plot with dimensions**

Compacting (Fig. 9a) the section around the explosion centre (0.5 - 1 m) enables clear contours of the movements (Fig. 8a). The explosion keeps a nearly spherical shape till 0.004 s after ignition with a flame speed of 185 m/s (Fig. 9) and moves downstream (the fireball) at a velocity of 87.9 m/s (Fig. 10a). A flame propagates upstream (Fig. 8b) with a velocity of 151 m/s (Fig 10 b).

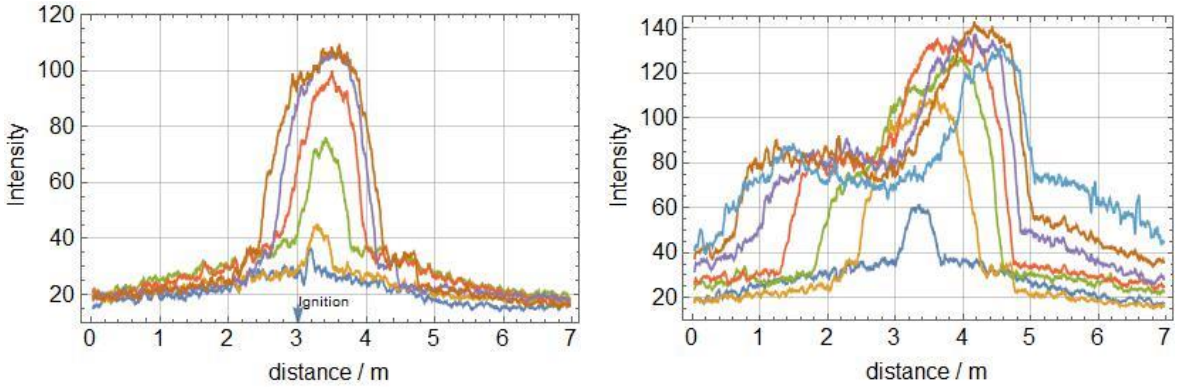


(a) (b)

**Figure 8: (a) Explosion on ignition, time steps 0.67 ms, (b) upstream propagation, steps of 3.3 ms.**

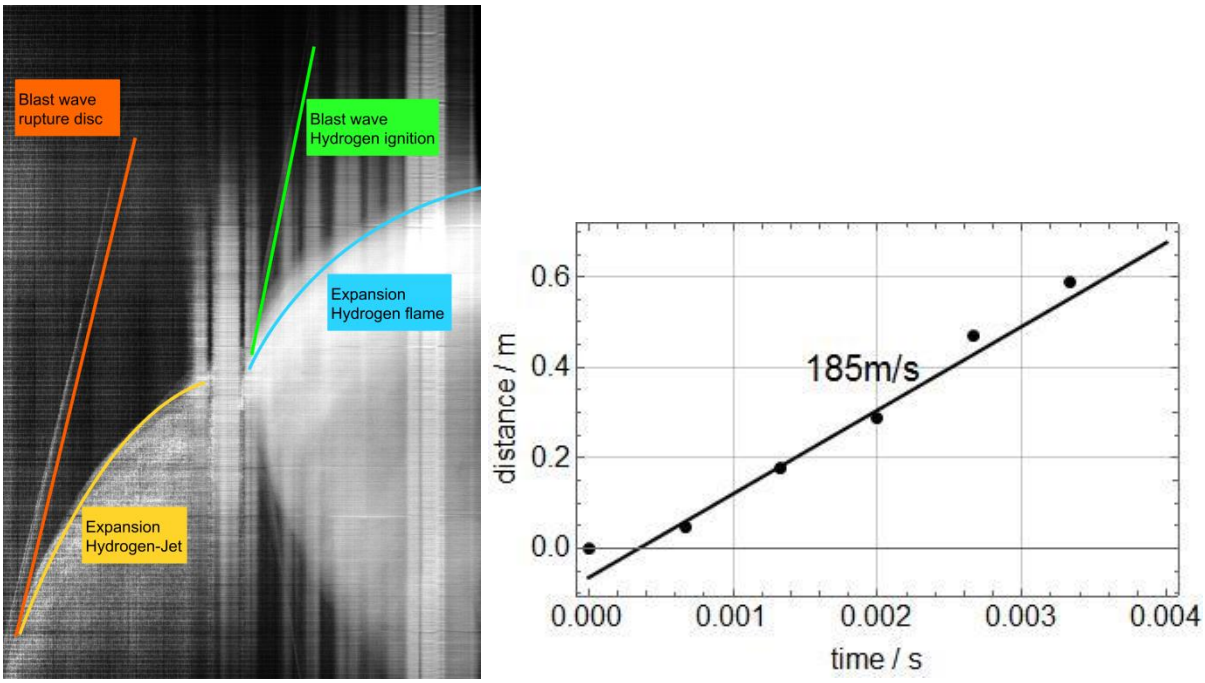


(a) (b)

**Figure 9: (a) overview on the movement: all images in the sequence compacted, (b) flame velocity of the explosion.**

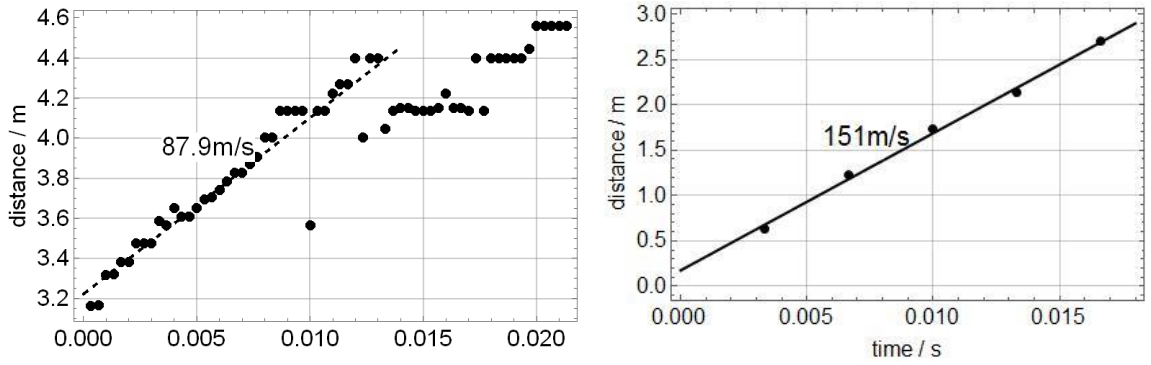


(a) (b)

**Figure 10: (a) Downstream movement of maximum intensity of the fire ball (b) flame velocity of upstream front.**

### 3.2.2 "Normal" Reaction

The "normal" reaction, which means that it is not far away from spherical premixed explosions to be presented in more detail, was initiated by an ejecting jet from a 20 MPa reservoir. The hydrogen air turbulent mixed jet ignited at a glow plug of 950 °C in a distance of 5 m from the nozzle (see Table 3, H63). For these experiments no shock waves were observed. Fig. 11 shows a sequence of images starting with the ignition and ending up with an advanced upstream flame. The visibility is low as mainly despeckled images can be evaluated.

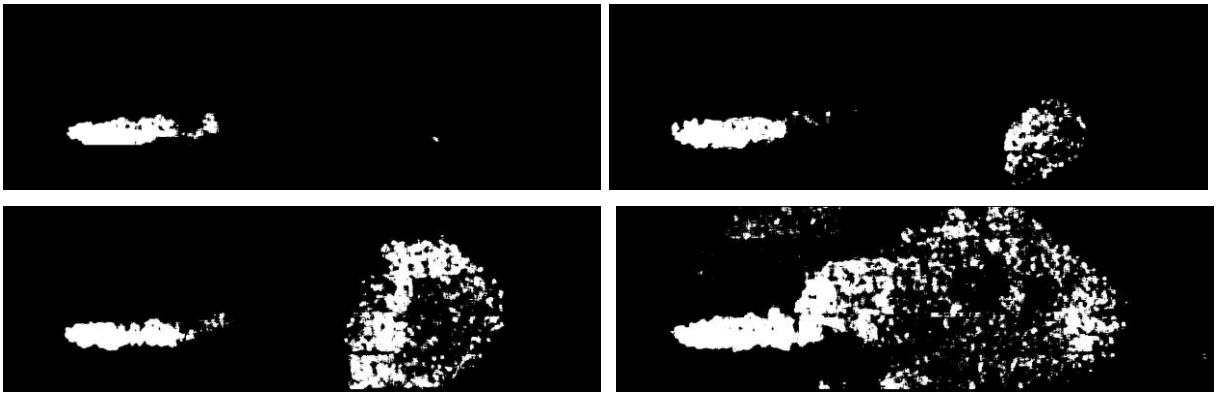

**Figure 11: Sequence of images starting with ignition, followed by three images with time steps of 0.013 s showing the explosion development from ignition, beginning upstream propagation and advanced upstream flame propagation (0.1 s).**

After 0.1 s, the jet covers the glow plug and reacts with a delay from the first indication of ignition of 0.001-0.002 s. Fig. 11 shows the reaction evolving after 0.0333 s. Non-reacted parts of the jet move on. They form the later medium for the gas explosion. At first the gas explosion seems to stay at about the same position for 0.067 s. Then it drifts downstream and a flame front propagates towards the jet orifice (see Fig.12). The flame velocities are derived from the pictures in Fig. 12 measuring the distances between the main peak flanks or the progression of the successive front. The resulting velocities are given in Fig. (13).

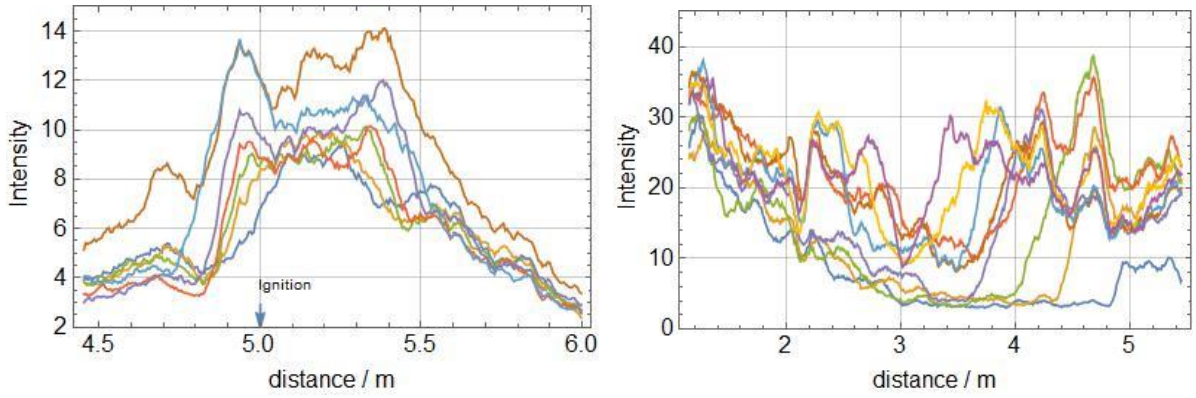


(a) (b)

**Figure 12: (a) Compacted contours of the explosion progress in steps of 0.00133 s. (b) Contours of upstream flame propagation in steps of 0.0067 s. After 0.05 s at 2 m an explosion occurs this delays the upstream propagation and mixes up with the upstream flame.**

The flame velocity of 24 m/s of the explosion is closely above that of spherical gas explosions and therefore is named here "normal".

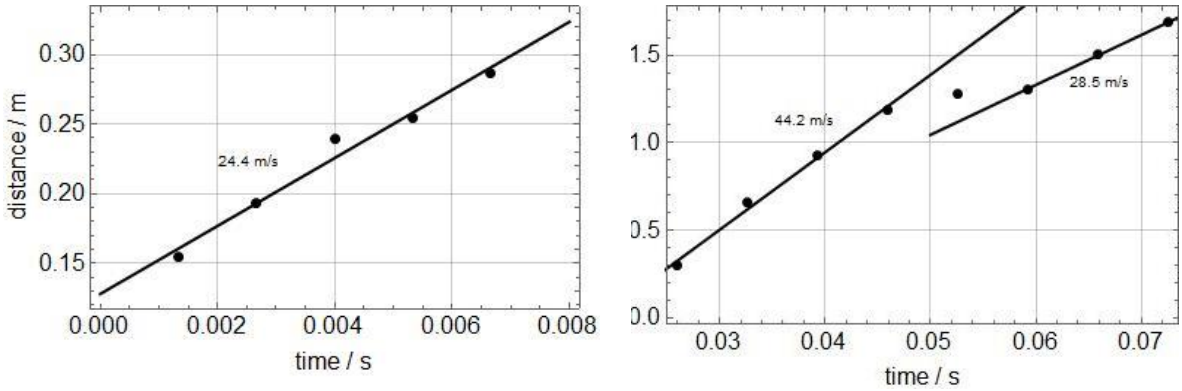


**(a)** **(b)**

**Figure 13: (a) Flame velocity of the explosion. (b) Flame velocity running upstream which is delayed when the explosion at 2 m occurs.**

### 3.2.3 "Weak" reaction

The weak reaction is nearly invisible. Therefore only despeckled images are presented (Fig 4). The "weak" reaction, which means, that it is not below the effects of spherical premixed explosions. The presented results were obtained from an ejecting jet from a 20 MPa reservoir. The hydrogen air turbulent mixed jet ignited at a glow plug with temperature 850 °C, the glow plug was mounted in a distance from the nozzle of 7 m (see Table 4, H71). For these experiments no shock waves were observed. Fig. 14 shows an image starting with completed explosion.

**Figure 14: Full view (2.2 m x 7.1 m) on the jet behind the orifice and the explosion occurs 0.1 s after ignition at the glow plug of 850 °C.**

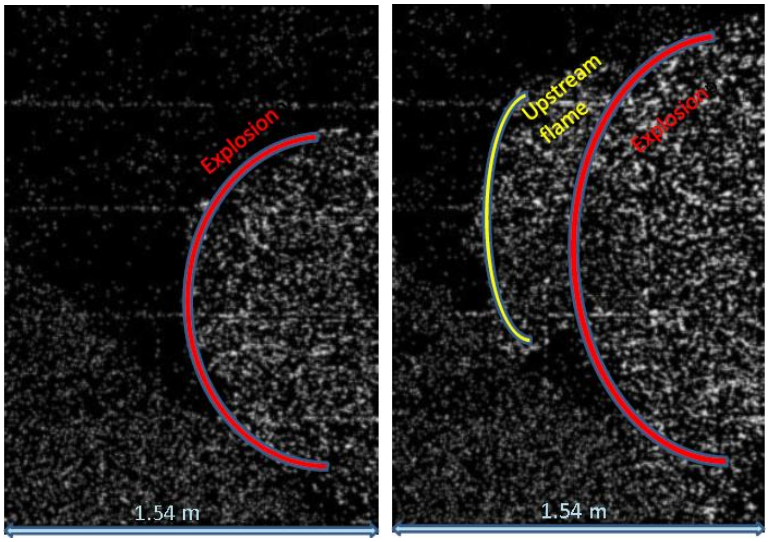


(a) (b)

**Figure 15: (a) Explosion after 0.047 s, (b) End of explosion and upstream propagation of the flame after 0.1667 s.**

Compacted images gave the curves of the progress of reaction given in Fig. 16. These figures enable the access to the flame velocities, although the fireball is not comletely in the field of view. Fig. 17 shows the velocities. With 11 m/s, the flame velocity of the explosion is well below the one of a spherical explosion. The upstream flame propagation stopped about 1.2 m upstream the igniting source and then drifts downstream.

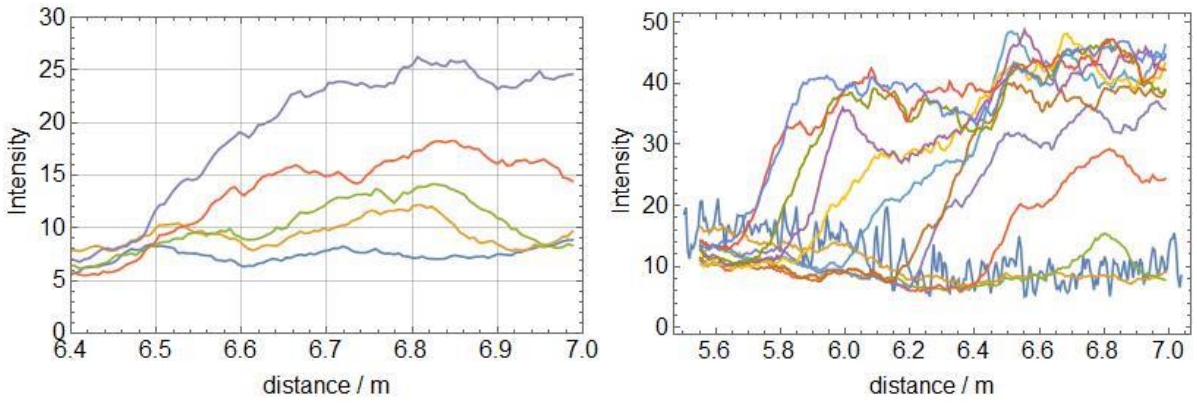


(a) (b)

**Figure 16: (a) Compacted contours of the explosion progress in steps of 0.0133 s. (b) Contours of upstream flame propagation in steps of 0.02 s. After the red and blue profiles the fireball drifts downstream, when reaching 5.6 m.**

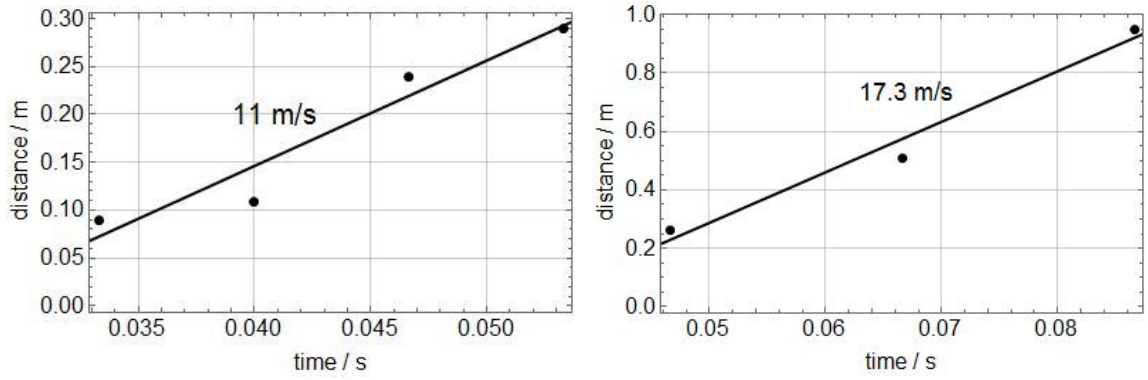


(a) (b)

**Figure 17: (a) Flame velocity of the explosion. (b) Flame velocity upstream.**

### 3.3 Spectroscopy and evaluation

The emission spectroscopy in the NIR wavelength range shows the occurrence of water by the water bands between 1.3 and 2.2 µm and therefore the occurrence of a reaction between the hydrogen jet and the ambient air [24]. The entrained air can be estimated by analysing the $CO_2$ emission in the middle infrared range (MIR) at 4.2 µm. This was investigated in a former study [24]. Further hydrogen/air flame radiation research also for turbulent flames can be found in Ref. [23].

Here the spectra in the NIR were analysed by a least squares fit method which fits a model spectrum of calculated $H_2O$ band system to experimental spectrum [25]. The resulting fit parameters are the temperature of the $H_2O$ band system. An example fit of the water band system at 1.3 µm is shown in Fig. 18a.

The evolution in time of temperature and the integral intensity of the water band system for the "strong" and "normal" reaction of hydrogen jets (experiment H51 "strong" and H63 "normal") are depicted in Fig. 18b-18c. There the zero point of time is the start time of reaction where the hydrogen jet was ignited at the glow plug. In the case of "weak" reaction the radiation of the reacting hydrogen jet was too low for emission spectroscopy measurements.

The resulting temperatures for the "strong" reaction experiment (Fig. 18b, black line) are in the temperature range between 2000 and 2200 K due to the gas explosion. They are comparable to former measurements [27]. In the case of "normal" reaction the temperatures are first at 1900 K till it increase up to 2100 K after 200 ms where the gas explosion seems to stay at the same position (cf. Fig. 12). Both temperature profiles show oscillations with a low and higher frequency. The higher frequency oscillations are also visible in the integral intensity (Fig. 18 c). Probably it is an effect of the turbulent combustion process.

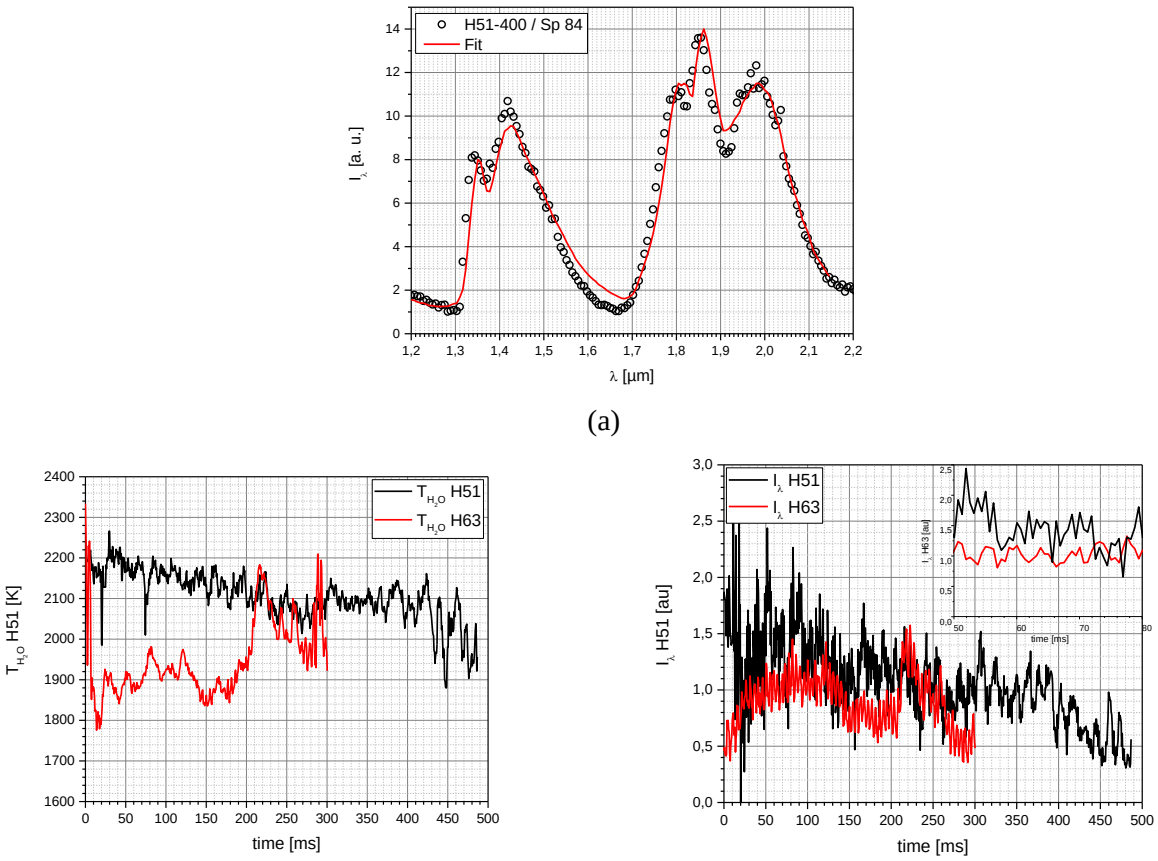


**Figure 18: Example fit of emission spectrum in the NIR of the water bands (a). Temperature profile (b) and integral intensity (c) of "strong" and "normal" reaction.**

## 4 Conclusions

On hitting hot devices, the transient jets evolve with high turbulence depending on the configuration of the nozzle and especially the pressure in the hydrogen reservoir. In addition the length of the jets and the flames generated by ignition at a hot surface varies. Parameters to be varied were initial pressure of the source (2.5, 10, 20 and 40 MPa), distance between the nozzle and the hot surface (3, 5 and 7 m) and temperature of the hot surface (between 400 and 1000 K). The interaction of the hydrogen jets is visualized by high-speed cinematography techniques and high-speed NIR spectroscopy was used to obtain temperature profiles of the expanding deflagrations. The jets ignite already above 450 K for conditions mainly from the tubular source of 40 MPa. In addition, the propagation of the flame front depends on all three varied parameters: temperature of the hot surface, the pressure in the reservoir and the distance between nozzle and hot surface. It can be separated into "strong" reactions which generate shockwaves and deflagrate at velocities well above 100 m/s, "normal" reactions show a similar behaviour like premixed stoichiometric spherical hydrogen air explosion and "weak" reactions are well below. In most cases also upstream propagation occurs. A high turbulence seems to lead to the strong deflagrations. At high temperatures of the ignition source, the interaction leads to fast deflagration speeds up- and downstream of the jet. The temperature profiles enable an estimation of the radiation emission.

## 5 References


1. Kotchourko, A., Baraldi, D., Bénard, P., Eisenreich, N., Jordan, T., Keller, J., Tchouvelev, A., State of the art and research priorities in hydrogen safety, *Joint Research Centre of the European Commission (JRC)*, 2014.
2. Bragin, M. V., Molkov, V. V., Physics of spontaneous ignition of high-pressure hydrogen release and transition to jet fire, *International Journal of Hydrogen Energy*, *36*(3), 2589-2596, 2011.
3. Yamada, E., Kitabayashi, N., Hayashi, A. K., Tsuboi, N., Mechanism of high-pressure hydrogen auto-ignition when spouting into air, *International Journal of Hydrogen Energy*, *36*(3), 2560-2566, 2011.
4. Pehr K., Aspects of safety and acceptance of LH2 tank systems in passenger cars, *International Journal of Hydrogen Energy*, 21, 387 – 395, 1996.
5. Astbury, G.R., Hawksworth, S.J., Spontaneous ignition of hydrogen leaks: a review of postulated mechanisms, *Proceedings of the First International Conference on Hydrogen Safety*, Pisa, Italy, 8-10 Sep 2005.
6. Mogi, T., Horiguchi, S., Experimental study on the hazards of high-pressure hydrogen jet diffusion flames, *Journal of Loss Prevention in the Process Industries*, 22, 45-51, 2009.
7. Deimling, L., Weiser, V., Blanc, A., Eisenreich, N., Billeb, G., Kessler, A., Visualisation of jet fires from hydrogen release, *International Journal of Hydrogen Energy*, 36, 2360-2366, 2011.
8. Kessler, A., Schreiber, A., Wassmer, C., Deimling, L., Knapp, S., Weiser, V., Eisenreich, N., Ignition of hydrogen jet fires from high pressure storage, *International Journal of Hydrogen Energy*, *39*(35), 20554-20559, 2014.
9. Eckl, W., Eisenreich, N., Herrmann, M.M., Weindel, M., Emission of radiation from liquefied hydrogen explosions, *Chemie Ingenieur Technik*, 67, 1015-17, 1995.
10. Veser, A., Kuznetsov, M., Fast, G., Friedrich, A., Kotchourko, N., Stern, G., Breitung, W., The structure and flame propagation regimes in turbulent hydrogen jets, I*nternational Journal of Hydrogen Energy*, *36*(3), 2351-2359, 2011.
11. Ruggles, A. J., Ekoto, I. W., Ignitability and mixing of underexpanded hydrogen jets, *International Journal of Hydrogen Energy*, *37*(22), 17549-17560, 2012.
12. Rudy, W., Teodorczyk, A., Wen, J., Self-ignition of hydrogen–nitrogen mixtures during high-pressure release into air. *International Journal of Hydrogen Energy*, 2016.
13. Bie, H., Hao, Z., & Ye, J., Numerical Investigation of Nozzle Aspect Ratio Effects on Hydrogen Jet Release Characteristics. In *ASME 2016 Pressure Vessels and Piping Conference* (pp. V01BT01A029-V01BT01A029). American Society of Mechanical Engineers, July 2016.
14. Jang, C. B., Choi, S. W., Simulation and damage analysis of an accidental jet fire in a high-pressure compressed pump shelter. *Safety and health at work*, *8*(1), 42-48, 2017.
15. Jang, C. B., & Jung, S., Numerical computation of a large-scale jet fire of high-pressure hydrogen in process plant. *Energy Science & Engineering*, *4*(6), 406-417, 2016.
16. Jang, C. B., Choi, S. W., Baek, J. B. CFD modeling and fire damage analysis of jet fire on hydrogen pipeline in a pipe rack structure. *International Journal of Hydrogen Energy*, *40*(45), 15760-15772, 2015.
17. Sakamoto, J., Sato, R., Nakayama, J., Kasai, N., Shibutani, T., & Miyake, A., Leakage-type-based analysis of accidents involving hydrogen fueling stations in Japan and USA. *International Journal of Hydrogen Energy*, *41*(46), 21564-21570, 2016.
18. Dorofeev, S.B., Efimenko, A.A., Kotchurko, A.S., and Chaivanov, B.B., Evaluation of the hydrogen explosions hazard, *Nuclear Engineering Design*, 148:305-316, 1995.
19. Dorofeev, S.B., Kuznetsov, M.S., Alekseev, V.I., Efimenko, A.A., Breitung, W., Evaluation of limits for effective flame acceleration in hydrogen mixtures, *Journal of Loss Prevention in the Process Industries* 14, 583–589, 2001.
20. Raffel M., Richard H., Meier G.E.A, On the applicability of Background Oriented Optical Tomography, *Experiments in Fluid*, 447-481, 2000.
21. Richard H., Raffel M., Rein M., Kompenhans J., Meier G.E.A., Demonstration of the applicability of a Background Oriented Schlieren (BOS) method, *10$^{th}$ Symposium of Applications Laser Techniques to Fluid*, 2000.

22. Keßler, A., Ehrhardt, W., Langer, G., Hydrogen detection: Visualisation of Hydrogen Using Non Invasive Optical Schlieren Technique BOS, *1st International Conference on Hydrogen Safety*, Pisa, Italy, September 8-10, 2005.
23. Gore J., Jeng S., Faeth G., Spectral and total radiation properties of turbulent hydrogen/air diffusion flames, *Journal of Heat Transfer*, 109, 165–171, 1987.
24. Kessler, A., Wassmer, C., Knapp, S., Weiser, V., Sachsenheimer, K., Raab, A., Langer, G., Eisenreich, N., Effects of radiation on the flame front of hydrogen air explosions, *6th International Conference on Hydrogen Safety*, Yokohama (Japan), October 19-21, 2015.
25. Weiser, V., Eisenreich, N., Fast Emission Spectroscopy for a Better Understanding of Pyrotechnic Combustion Behaviour, *Propellants, Explosives, Pyrotechnics*, 30, 67-78, 2005.
26. Abramovich, G. N., The Theory of a Free Jet of a Compressible Gas, Technical Memorandum National Advisory Committee for Aeronautics No. 1058, March 1944.
27. Kessler, A., Schreiber, A., Deimling, L., Weiser, V., Klan, T., Billeb, G., Knapp, S., Eisenreich, N., Radiation from Hydrogen Jet Fires Investigated by Time-Resolved Spectroscopy, *5th International Conference on Hydrogen Safety*, Brussels, Sept 2013.